Accurate appearance-based visualization of car paints

Ivo van der Lans, Eric Kirchner, André Half, AkzoNobel Automotive & Aerospace Coatings, Sassenheim, the Netherlands.

Abstract

We propose a new method to generate images with a given color and texture, in order to visualize the appearance of car paints. Unlike current methods, the new method is based on visual comparisons of rendered paints with actual physical samples. Thus, we optimized the method to maximize the appearance match between rendered image and the corresponding car paint. In the new method it is possible to set accurate numerical values for not only color properties, but also for well-defined texture parameters.

The new method is able to accurately render car paints under various light conditions, ranging from purely unidirectional, intense spot light to purely diffuse light. We show that the latter type of lighting conditions, which is often encountered in practical situations, is not well covered by existing rendering techniques that are based on BRDF and BTF measurements. Compared to existing methods for rendering, the proposed method is much faster regarding measurement and calculation, it has lower instrument costs and requires less data storage.

Texture in car paints

In modern car paints, the observed color changes with the viewing and illumination geometry. But these paints also show another striking visual aspect [1]. When viewed from about a meter or less, the color of the paint appears to be not uniform. This phenomenon of texture, and various other visual aspects of car paints, was described by McCamy in two pioneering articles [2][3]. The importance of texture in the visual appearance of car paints was recently emphasized by the Commission Internationale de l'Eclairage (CIE) [4].

In our own work, we extended these ideas. We introduced new concepts with clear definitions for describing texture [5]. Depending on the type of lighting, different aspects of texture are visible. Under diffuse illumination, Diffuse Coarseness is observed. It is the perceived contrast in the irregular light/dark pattern exhibited by car paints viewed under such diffuse illumination conditions. But under intense unidirectional lighting, the observed texture is completely different. Glint Impression is the overall impression of several or many tiny light-spots (glints or sparkles) that are strikingly brighter, or differently colored, as compared to their surroundings.

In psychophysical tests we have quantified both texture phenomena [5]. Based on this research, and in cooperation with BYK Gardner GmbH and Merck KGaA, a new instrument was developed that is able to measure not only color with a multi-angle spectrophotometer, but also both texture parameters [6][7]. This instrument is now commercially available from BYK Gardner under the name BYK-mac®. It is also actively used in our more recent research on color differences and texture differences between paint samples [8][9].

Previous work on rendering car paint

Methods and software for 3D rendering of car paints are widely available for several years now [10][11]. Although many of these methods produce striking images, they are often not realistic [12], and the accuracy is not good enough for critical applications such as automobile design [13].

While the traditional approach to rendering utilized ray tracing [14], for rendering metallic paints this method is computationally too expensive for many applications. More recent methods to render color are based on the concept of the Bidirectional Reflectance Distribution Function (BRDF). This function combines a large number of reflectance values for a wide range of illumination and detection angles. Approaches where the BRDF is measured require expensive instruments and storing large amounts of data. For the latter reason, often the measured BRDF is fitted to parametric functions such as the Cook-Torrence model [15], or to non-parametric functions [16]. Obviously, the fitting functions are only an approximation to the measured BRDF.

Instead of measuring the BRDF some investigators use simplified physical models to calculate it. An early example is the work of Hanrahan *et al.* [17][18], whereas Ershov, Ďurikovič and co-workers provide a more recent example [19][20][21]. However, the "fast model of BRDF of a two-layer paint" that is used by Ershov *et al.* [19], is only a crude description of a modern car paint. It assumes that conventional absorption pigments and flake pigments occur in separated layers, which is very rare in practice. As a consequence, the occurrence of sparkles with different degrees of coloring which is easily seen in actual car paints is not accounted for in this model.

For rendering texture, a measurement technique similar to what is used for the BRDF was introduced by Dana *et al.* [14]. The paint sample is lit by a directional light source and photographed from different directions. The resulting images are combined in the Bidirectional Texture Function (BTF). This technique requires expensive acquisition systems and many hours of measurement times [22]. The size of the resulting BTFs is considerable, at around a gigabyte. No optimal compression algorithm was found yet, which hampers industrial applications.

Instead of using measurements, texture can also be simulated by statistically adding highlights to the pre-calculated image. This approach was pioneered by Ershov, Ďurikovič *et al.* [23][24][25][26]. With these techniques, impressive rendering for car paints can be obtained. A disadvantage of this approach is that it requires dozens of parameters.

For rendering both color and texture, Günther *et al.* used fit functions to the BRDF combined with a modification of Ershov's description of sparkle [12]. In a recent work published by Rump *et al.*, the same approach was taken, but sparkle was accounted for by measuring the BTF [27]. Although this approach leads to impressive simulations of the appearance of car paints, it requires measuring and storing ten thousands of images for each car paint. Even after compression, this requires 500 Mb of data. The computation time that is needed in this approach is also substantial, making real-time rendering difficult to achieve.

A new approach to rendering car paints

We base our color rendering on reflection measurements. To avoid excessive computation time and storage costs related to using the BRDF, we follow the approach taken by Meyer *et al.* and Dumont-Bècle *et al.*, and fit data from multi-angle reflection measurements taken under only a handful of different geometries [28][29][30]. This agrees with standard practice in automotive and in paint industry, where metallic paints are known to be characterized by reflection measurements under three different geometries [31][32]. Three more geometries are added to also characterize pearlescent coatings [33].

With the development of the BYK-mac®, it is now possible to use accurate measurement of texture as input to render textured surfaces such as car paints. In the development of the BYK-mac®, we developed image analysis methods to extract coarseness [34] and glint [35] data from digital images taken from car paints. With the insights thus developed, we investigated how to realize the reverse process, *i.e.* to generate digital images corresponding to a specified texture value. Our results for coarseness [34][36] showed that such rendered textures may correlate well with visual judgments on the corresponding physical samples [37]. In the present work, we develop an accurate method to generate digital images of car paints, with specified values for both diffuse coarseness and glint impression.

The simplest method to generate textured images is to superimpose a textured, grey-valued image over an image with a uniform color. A well-known disadvantage of this technique is that the color of the resulting, textured image will appear different from the color of the original uniform image [38][39][40]. The new approach aims at the accurate generation of images with predefined color and texture, making it possible to independently set the color and texture properties of the generated images.

In order to generate accurate digital images with prescribed color and texture, the target image is composed from three intermediate images: a grey-scale image of prescribed diffuse coarseness value, a grey-scale image of prescribed glint impression, and a colored image with the prescribed color. This approach has the additional advantage of being able to account for the distance between the observer and the painted object, because we found that the diffuse coarseness image and the glint impression image each require a different method to account for the observation distance.

Generation of grey-scale images with prescribed diffuse coarseness

The core algorithm to generate a grey-scale image with a prescribed value c of the diffuse coarseness is based on the following stochastic process. A digital image is regarded as a two-dimensional array of pixel values. Initially, the digital image is filled with zeroes. Its size is taken slightly larger than the size ultimately needed.

A patch is defined as a set of pixel values that are assigned to a square-shaped subsection of the total digital image. The patch itself does not have to be square shaped, but it can be generated in any useful form, such as the form of a point spread function.

The patch is then repeatedly generated on random positions in the target image, allowing overlap between the patches. Four different parameters define this process:

size: the size of each patch,

grey level: the intensity of the patch,

count: the number of patches that are generated (count is the average number of generated patches centered on each pixel).

sparkler: By putting a patch in the image, the values of the patch are added to the pre-existing values. After that, the whole pattern is multiplied by the value of the sparkler parameter. Subsequently, all pixel values of the image are renormalized to ensure no values exceed the maximum grey value.

We found that in order to generate images with a prescribed value c of diffuse coarseness, each of these four parameters needs to be described by a separate function that depends only on the value c.

$$\begin{pmatrix} size \\ gray\ level \\ count \\ sparkler \end{pmatrix} = \begin{pmatrix} f(c) \\ g(c) \\ h(c) \\ k(c) \end{pmatrix} \tag{1}$$

Here, functions *f(c)*, *g(c)*, *h(c)* and *k(c)* are introduced. We found good results when we used the following expressions for these functions:

$$\begin{aligned} f(c) &= A_f + B_f \cdot [c]^{C_f} \\ g(c) &= A_g + B_g \cdot [c]^{C_g} \\ h(c) &= A_h + B_h \cdot [c]^{C_h} \\ k(c) &= A_k + B_k \cdot [c]^{C_k} \end{aligned} \tag{2}$$

With these definitions, the stochastic algorithm is able to generate grey-scale images that are very similar to the digital images produced internally by the BYK-mac®.

This similarity was exploited further by using BYK-mac® images taken from the so-called anchor panels described in an earlier publication [5]. In these car paint samples the value for diffuse coarseness systematically varies from very small to very large, whereas the measured reflection curves for these samples remain almost constant. By basing the optimization of the fit parameters on BYK-mac® images of these anchor panels, we make sure that the generated diffuse coarseness images all refer to the same grey color. This is illustrated in Figure 1.

The values of the parameters A_f, B_f through C_k in equation (2) were fitted such that the resulting images showed optimum similarity with the BYK-mac® images taken from the anchor panels. The similarity between generated and measured images was numerically expressed in terms of statistical properties of the intensity histograms of these images. Our analysis was based on the median value, average value, and the 10, 20, 30 up to 90 percentile values. The squared sum of differences in each of these statistical properties was minimized, resulting in optimum values for the parameters A_f, B_f through C_k.

In this way, grey-scale images with prescribed diffuse coarseness were generated. In a visual test the accuracy of this method was confirmed, as observers were not able to distinguish the images produced by the BYK-mac® and those generated with the stochastic algorithm.

Generation of grey-scale images with prescribed glint impression

The core algorithm to generate a grey scale image with prescribed value g for glint impression is very similar to the core algorithm just described for generating images with

prescribed diffuse coarseness. Again, the same four parameters are needed, but in this case these parameters obviously depend on the prescribed value of glint impression

$$\begin{pmatrix} size \\ gray\ level \\ count \\ sparkler \end{pmatrix} = \begin{pmatrix} m(g) \\ n(g) \\ p(g) \\ q(g) \end{pmatrix} \tag{3}$$

where in this case for the functions *m(g)*, *n(g)*, *p(g)*, and *q(g)* we found best results when using transformed functions, inspired by the Fermi-Dirac distribution function:

$$\begin{aligned} m(g) &= 1 + 100 / \left(1 + \exp\left[A_f + B_f \cdot [g]^{c_f}\right]\right) \\ n(g) &= 1 + 100 / \left(1 + \exp\left[A_g + B_g \cdot [g]^{c_g}\right]\right) \\ p(g) &= 1 + 100 / \left(1 + \exp\left[A_h + B_h \cdot [g]^{c_h}\right]\right) \\ q(g) &= 1 + 100 / \left(1 + \exp\left[A_k + B_k \cdot [g]^{c_k}\right]\right) \end{aligned} \tag{4}$$

Very similar to the previous case, the optimum values of the parameters A_f , B_f through C_k were found by statistically comparing the generated images with images measured by the BYK-mac® instrument, on the corresponding anchor panels (Figure 2).

Combining colored and textured images

Each of the textured images (referring to either the diffuse coarseness image or the glint impression image) is then separately combined with a uniformly colored image. The latter image is generated, based on spectrophotometric reflectance measurements. With the standard methods from the sRGB system, an image is constructed with pixel color values (R_m, G_m, B_m) representing the prescribed color.

The algorithm described above has assigned a grey-value *G* to each pixel of the glint impression image, which obviously depends on the geometry γ it refers to. If we denote the *G* value averaged over all pixels as $\overline{G}$, then a first correction for color differences usually resulting from generating textured images is defined by subtracting this average value $\overline{G}$ from the *G* value of each particular pixel. Normalizing the resulting pixel values in the image, we thus define the following intermediate image, which is a colored version of the grey-scale glint impression image:

$$\begin{aligned} R_{sa}(\gamma,x,y) &= Max\left(0,\ Min\left[R_m(\gamma) + G(\gamma,x,y) - \overline{G}(\gamma)\ \right]\right) \\ G_{sa}(\gamma,x,y) &= Max\left(0,\ Min\left[G_m(\gamma) + G(\gamma,x,y) - \overline{G}(\gamma)\ \right]\right) \\ B_{sa}(\gamma,x,y) &= Max\left(0,\ Min\left[B_m(\gamma) + G(\gamma,x,y) - \overline{G}(\gamma)\ \right]\right) \end{aligned} \tag{5}$$

In this way, the resulting image not only preserves the prescribed color properties, but it also has the prescribed glint impression value. This is not only realized by subtracting the average $\overline{G}$ value described above, but also by the way the anchor panels were used in optimizing the stochastic algorithm.

For the diffuse coarseness images, the combination with the colored image proceeds in a very similar way.

$$\begin{aligned} R_{sd}(\gamma,x,y) &= Max\left(0,\ Min\left[R_{md} + C(x,y) - \overline{C}\right]\right) \\ G_{sd}(\gamma,x,y) &= Max\left(0,\ Min\left[G_{md} + C(x,y) - \overline{C}\right]\right) \\ B_{sd}(\gamma,x,y) &= Max\left(0,\ Min\left[B_{md} + C(x,y) - \overline{C}\right]\right) \end{aligned} \tag{6}$$

In this case, the parameters R_{md}, G_{md} and B_{md} refer to pixel values in the red, green and blue channel, generated in the case of diffuse lighting of an object with prescribed color. Also here, the accuracy of the algorithm was verified by using anchor panels.

Combining all images

In a final step, all images are combined in a way that best corresponds to the lighting situation that needs to be rendered. We found that simple linear interpolation gives a good rendering of effect paints in realistic conditions. We assume that the practical lighting conditions of the object can be described by a parameter *d*. A value *d=1* holds in case lighting is purely diffuse, while *d=0* signifies purely unidirectional lighting. Intermediate values refer to the situations in between these two extremes. With linear interpolation, we find

$$\begin{aligned} R(\gamma,x,y) &= Max\left(0,\ Min\left[1,\ R_{sd}(x,y)\times d + R_{sa}(\gamma,x,y)\times(1-d)\right]\right) \\ G(\gamma,x,y) &= Max\left(0,\ Min\left[1,\ G_{sd}(x,y)\times d + G_{sa}(\gamma,x,y)\times(1-d)\right]\right) \\ B(\gamma,x,y) &= Max\left(0,\ Min\left[1,\ B_{sd}(x,y)\times d + B_{sa}(\gamma,x,y)\times(1-d)\right]\right) \end{aligned} \tag{7}$$

In Figure 3, we show results for different combinations of values for diffuse coarseness and glint impression.

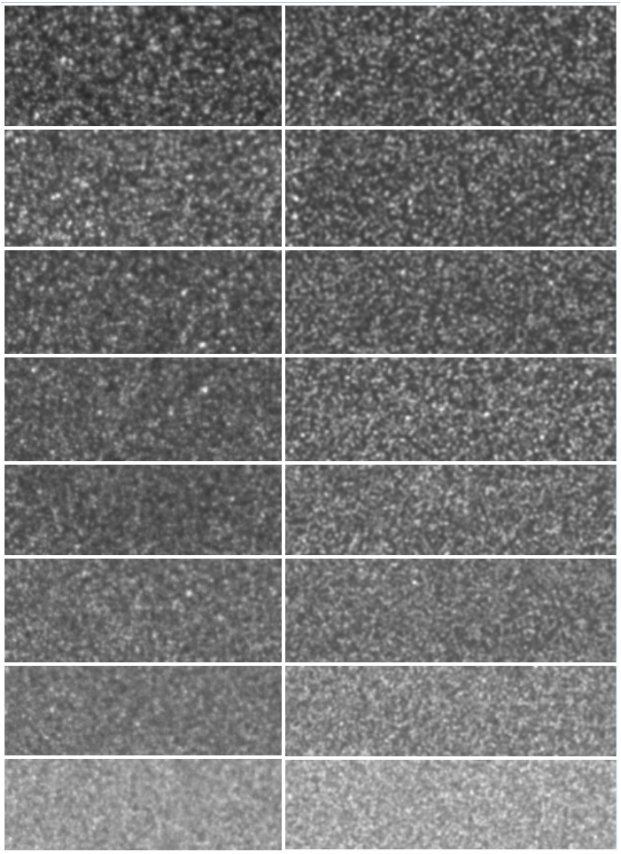

Figure 1. *Anchor panels, photographed under diffuse lighting conditions. From top to bottom, anchor panels have decreasing diffuse coarseness values. Left: images taken by digital camera from physical samples. Right: images produced by the algorithm described in the text.*

We found that the generated images become even more realistic when gloss is accounted for, by adding white reflection at and close to the specular angle. Also, images can be generated for curved objects as well, by interpolating color and

texture values corresponding to the respective geometries. For this interpolation, we found that cardinal spline functions gave the best results.

Visual testing the accuracy of rendering

With visual tests we tested the accuracy of the new rendering algorithms for car paints. With teams of observers, images of car paints produced by these algorithms were compared to physical samples with the same paint.

Several visual tests were conducted. First, the rendering of glints (sparkle) was tested by visually assessing flat samples under an intense spot light, and comparing them with images rendered on an LCD display. Although the dynamic range of an LCD display is not sufficient to render the full dynamic range of sparkle, our visual tests show that the rendering algorithm is successful in producing images from which paint samples with much sparkle can be distinguished from those with less sparkle.
In another test we rendered curved panels such as shown in Figure 4. In this representation, the aspecular angle is systematically varied from 0° to 110°. The resulting image looks like a strongly curved painted panel. Images like this were shown on an LCD display, and compared with cars that were painted with the corresponding paints. Obviously, the shape of cars is such that a wide range of aspecular angles is examined while observing them, and in the curved panel view we offer the possibility to examine this range. The cars were positioned one after another in an environment resembling a car repair bodyshop.

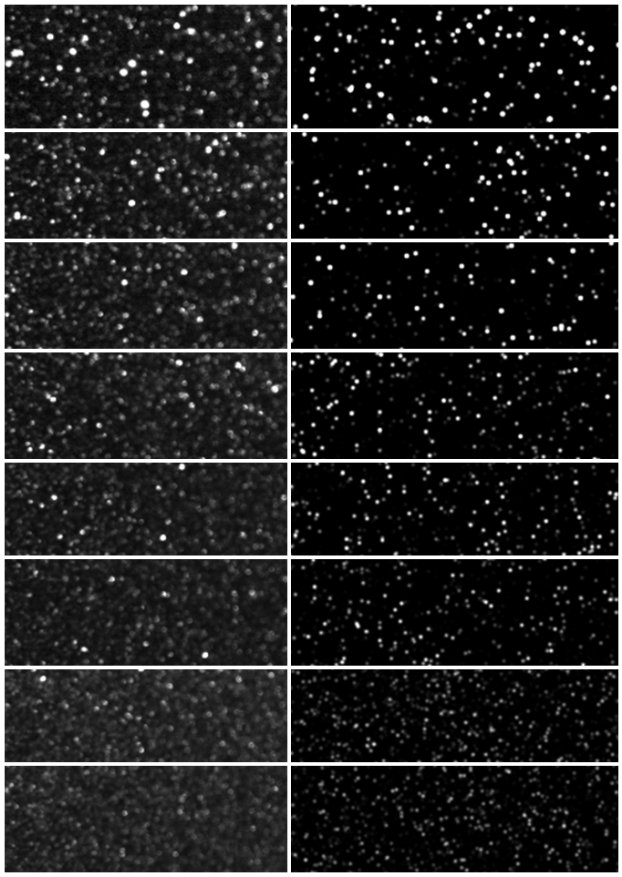

Figure 2. *Anchor panels, photographed under directional lighting. From top to bottom, anchor panels have decreasing glint impression values. Left: images taken by digital camera from physical samples. Right: images produced by the algorithm described in the text.*

First an initial test was carried out that was meant to determine the best values of parameters characterizing the lighting conditions surrounding the cars. We found relatively easily that the best results were found if we assumed that 70% diffuse and 30% directional light was present.

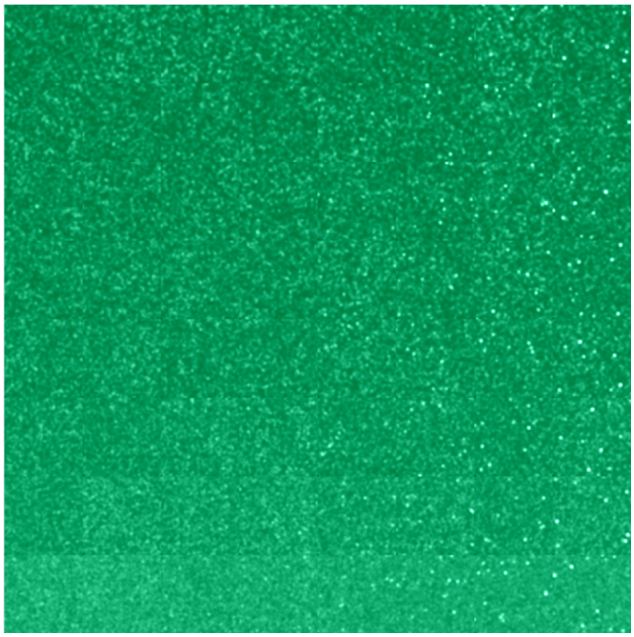

Figure 3. *Combination of color information with both diffuse coarseness and glint impression. While color remains fixed, glint impression increases in 8 discrete steps in horizontal direction. Similarly, diffuse coarseness increases from bottom to top.*

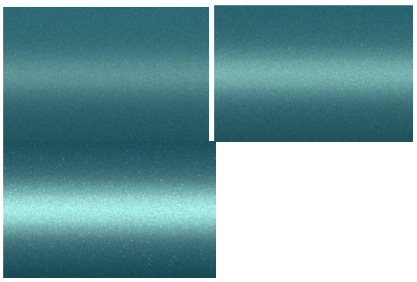

Figure 4. *Curved panel view for showing car paints, under different ratio's of diffuse : directional lighting (a) 75:25, (b) 70:30, (c) 30:70. (TOY774)*

In the main test, four observers assessed 21 different cars. These cars represented different types of car paints and covered a wide range of color categories for car paints: metallic grays, blue, red, green, purple and black. In this test, it was found that the type of texture seen under these lighting conditions is well rendered by the algorithms. Car paints with a coarser or a finer texture could be well distinguished by the algorithms.

Rendering of 3D objects

A small feasibility study was done on using the rendering algorithms on 3D objects. Figure 5 shows the results when we use a 3D model of the monkey nicknamed Suzanne, which is provided with the rendering software package 'Blender'. These images were calculated on a Core™2Quad Q9450 processor (2.66 GHz), requiring 1.5 seconds calculation time per image

for single threaded C# code. Thus we show that the proposed algorithms are feasible also for rendering 3D objects.

Discussion

In the proposed method, color and texture are measured in a way that is very short in time, and requiring much less computing time and data storage when compared with existing methods that are based on BRDF and BTF measurements. A disadvantage of this new method is that the rendered images are less likely to be very accurate for specific complex illumination conditions, than when global illumination models are used.

Our visual tests show that the rendered images compare well with physical samples carrying the corresponding car paints. These visual tests also show that the new rendering method is able to render car paints in different illuminant conditions, ranging from purely diffuse to purely directional lighting. When simulating practical situations, rendering at intermediate lighting conditions was found to be adequate as well. It is striking that in the rendering literature, visual comparisons between rendered images and the physical objects they are supposed to imitate are rarely made. In any case, our results confirm that the algorithms introduced here go beyond the target that seems to be set for many existing rendering techniques, which is to produce images that are visually pleasing.

For example, the images that we produce representing diffuse lighting show a type of texture, diffuse coarseness, that is hardly even mentioned in literature on rendering methods. This type of illumination, which occurs often in practical situations, is not adequately represented with BTF measurements. Although the number of digital cameras used in such measurements can be as large as a few hundred, such as in the work of Rump *et al.*[27], the angular resolution for the illumination and detection angles is quite crude when compared to the subtle angular effects of metallic flakes that need to have the right orientation for incident light to be reflected exactly towards the detector. In the rendering method proposed in the present work, these difficulties are avoided by characterizing the texture in a few measurable quantities, and interpolating their values to any required illumination and/or observation angle.

Another major difference between the proposed rendering algorithm and existing approaches is that the latter are either based on physical measurements or on physical modeling, rather than on directly accounting for the color and texture appearance as perceived by the human visual system. For example, in existing methods, no attempt is made to account for the finite resolution of the human eye. In our algorithm, calibration by visual examination is crucial at several phases of the development, hence ensuring that the visual appearance of (color and) texture of the car paint does match the physical samples as close as possible.

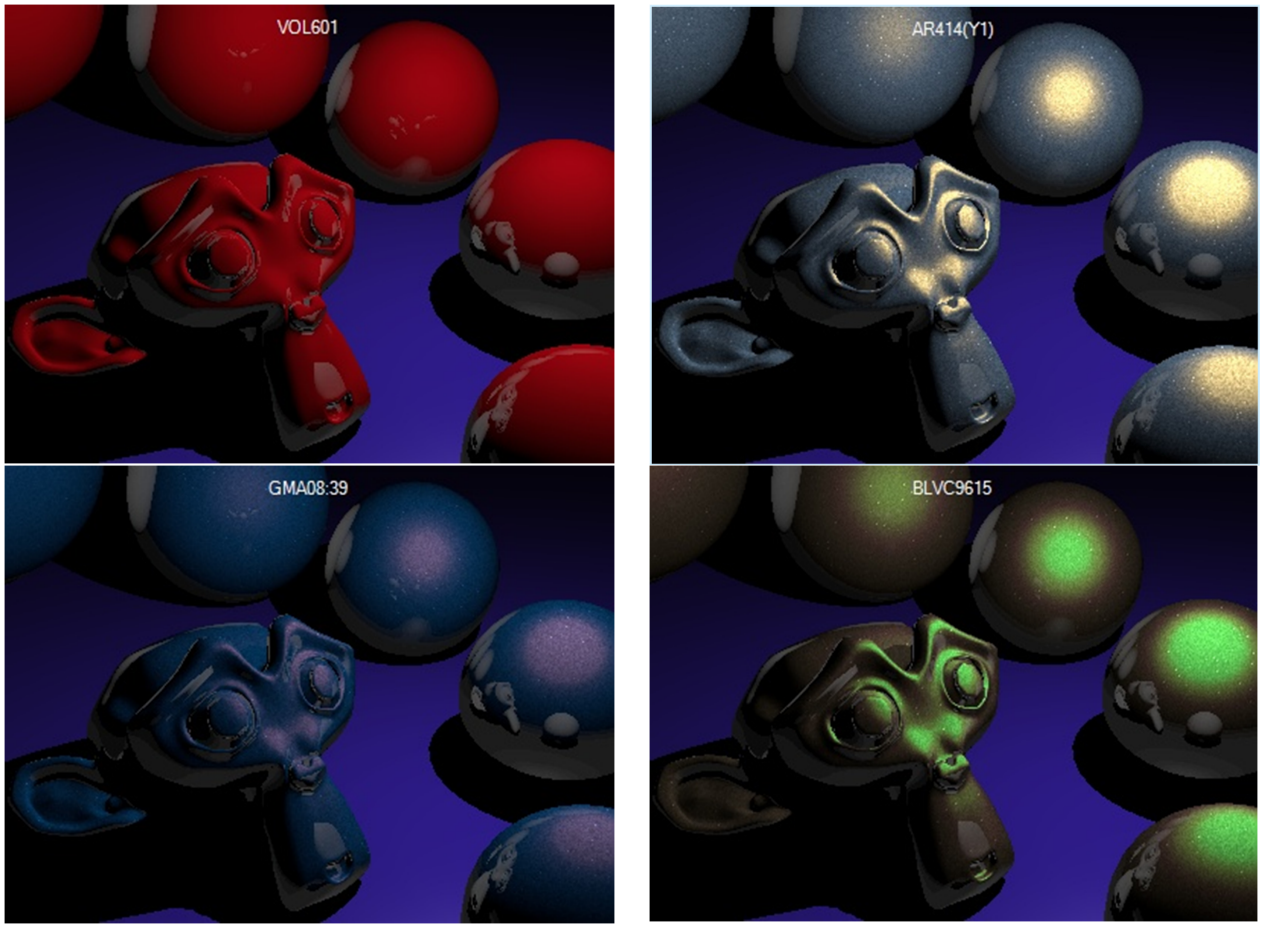

Figure 5. *Monkey Suzanne, rendered as if covered by four commonly used car paints (a) solid color "classic red" from Volvo 60 (2003), (b) three-layer pearl coating named Azzurro Nuvola, from Alfa Romeo Spider (2009), (c) metallic color Mystique Blue from Chevrolet Avalanche (2009), and (d) Shot Silk color, obtained by mixing metallic and pearlescent pigments, used for the Rover 25 (2004).*

References

[1] R.S. Hunter, "The modes of appearance and their attributes", in: J.J. Rennilson and W.N. Hale, eds., Review and Evaluation of Appearance: Methods and Techniques (American Society for Testing and Materials, Philadelphia, 1986) pg. 5–13.

[2] C.S. McCamy, "Observation and measurement of the appearance of metallic materials. I. Macro appearance", Color Res. Appl., 21, 292–304 (1996).

[3] C.S. McCamy, "Observation and measurement of the appearance of metallic materials. II. Micro appearance", Color Res. Appl., 23, 362–373 (1998).

[4] CIE Technical report 175:2006. A Framework for the Measurement of Visual Appearance. ISBN 3 901 906 52 5, pg. 55 (2006).

[5] E.J.J. Kirchner, G.J. van den Kieboom, S.L. Njo, R. Supèr and R. Gottenbos, "The Appearance of Metallic and Pearlescent Materials", Color Res. Appl., 32, 256-266 (2007).

[6] E. Kirchner, K. de Haas, L. Njo and M. Rösler, "Objectiv glitzern und funkeln", Farbe & Lack 114(2),32-36 (2008).

[7] E. Kirchner, L. Njo, K. de Haas and M. Rösler, "Coarseness and Glints", Eur. Coat. J., 11, 46-50 (2006).

[8] N. Dekker, E.J.J. Kirchner , R. Supèr, G.J. van den Kieboom and R. Gottenbos, "Total appearance differences for metallic and pearlescent materials: contributions from color and texture", Color Res. Appl., 36, 4-11 (2011).

[9] E.J.J. Kirchner, N. Dekker, R. Supèr, G.J. van den Kieboom and R. Gottenbos, "Quantifying the influence of texture on perceived color differences for effect coatings", Proc. 11th Congress of the International Colour Association (AIC), Sydney. (2009).

[10] H. Beckersjürgen, "Simulation und Visualisierung komplexer Oberflächen in Echtzeit", JOT/Oberfläche 41, 88-91, (Oct. 2001).

[11] I. Thomas, "Lacke am Computer designen", Farbe & Lack 107(11), 44-50 (2001).

[12] J. Günther, T. Chen, M. Goesele, I. Wald and H.P. Seidel, "Efficient acquisition and realistic rendering of car paint", in: G. Greiner, J. Hornegger, H. Niemann and M. Stamminger, eds., Proc. Vision, Modeling and Visualization (VMV'05), Erlangen, pg. 487-494. (2005).

[13] J.A. Ferwerda, S.H. Westin, R.C. Smith and R. Pawlicki, "Effects of rendering on shape perception in automobile design", Proc. ACM Symposium on applied perception in Graphics and Visualization, pg. 107-114. (2004).

[14] K.J. Dana, B. van Ginneken, S.K. Nayar and J.J. Koenderink, "Reflectance and texture of real-world surfaces", ACM Transactions on Graphics, 18(1), 1-34 (1999).

[15] R.L. Cook and K.E. Torrance, "A reflectance model for computer graphics", Proc. 8th Conference on Computer Graphics (SIGGRAPH) New York, pg. 307-316. (1981).

[16] D.B. Kim, M.K. Seo, K.Y. Kim and K.H. Lee, "Acquisition and representation of pearlescent paints using an image-based goniospectrophotometer", Optical Engineering, 49(4), 043604-1 – 13 (2010).

[17] P. Hanrahan and W. Krueger, "Reflection from layered surfaces due to subsurface scattering", Proc. 20th Conference on Computer Graphics (SIGGRAPH), New York, pg. 165-174. (1993).

[18] J. Dorsey and P. Hanrahan, "Modeling and rendering of metallic patinas", Proc. 23rd Conference on Computer Graphics (SIGGRAPH) New York, pg. 387-396. (1996).

[19] S. Ershov, K. Kolchin and K. Myszkowski, "Rendering pearlescent appearance based on paint-composition modeling", Eurographics 2001, Computer Graphics Forum, 20, C221–C238 (2001).

[20] R. Ďurikovič and T. Agoston, "Prediction of optical properties of paints", Centr. Eur. J. Phys., 5(3), 416-427 (2007).

[21] R. Ďurikovič, K. Kolchin and S. Ershov, "Rendering of Japanese artcraft", in: L. Navazo Alvaro and Ph. Slusallek, Eds., Short Presentations of EUROGRAPHICS Conference, Saarbrücken, pg. 131-138. (2002).

[22] G. Müller, J. Meseth, M. Sattler, R. Sarlette and R. Klein, "Acquisition, synthesis and rendering of bidirectional texture functions", Computer Graphics Forum (Eurographics), 24(1), 83-109 (2005).

[23] S. Ershov, A. Khodulev and K. Kolchin, "Simulation of sparkles in metallic paints", in: Proc. Graphicon'99 (Eurographics), pg. 121-128. (1999).

[24] R. Ďurikovič and W.L. Martens, "Simulation of sparkling and depth effect in paints", Proc. 19th Spring Conference on Computer Graphics SCCG'03, New York, pg. 193-198. (2003).

[25] S. Ershov, R. Ďurikovič, K. Kolchin and K. Myszkowski, "Reverse engineering approach to appearance-based design of metallic and pearlescent paints", The Visual Computer, 20, 586-600 (2004).

[26] R. Ďurikovič, "Explicit method of sparkling effect simulation", Proc. Human and Computer Conference - HC2002, Aizu-Wakamatsu, pg. 87-91. (2002).

[27] M. Rump, G. Müller, R. Sarlette, D. Koch and R. Klein, "Photo-realistic rendering of metallic car paint from image-based measurements", Computer Graphics Forum, 27 (2), 527-536 (2008).

[28] G.W. Meyer and C. Shimizu, "Computational automotive color appearance", in: L. Neumann, M. Sbert, B. Gooch and W. Purgathofer, eds., Computational Aesthetics 2005: Eurographics workshop on Computational Aesthetics in Graphics, Visualization and Imaging. (Eurographics association), Girona, 217-222. (2005).

[29] C. Shimizu, G.W. Meyer and J.P. Wingard, "Interactive goniochromatic color design", in: Proc. IS&T/SID's Eleventh Color Imaging Conference, Scottsdale, pg. 16-22. (2003).

[30] P. Dumont-Bècle, E. Ferley, A. Kemeny, S. Michelin and D. Arquès, "Multi-texturing approach for paint appearance on virtual vehicles", Proc. Driving Simulation Conference, Sophia Antipolis, pg. 123-133. (2001).

[31] D.H. Alman, "Directional color measurement of metallic flake finishes", Proc. Inter-Society Color Council Conference on Appearance, Williamsburg, pg. 53-56. (1987).

[32] H.J.A. Saris, R.J.B. Gottenbos and H. van Houwelingen, "Correlation between visual and instrumental colour differences of metallic paint films", Color Res. Appl., 15, 200-205 (1990).

[33] E.J.J. Kirchner and W.R. Cramer, "Making sense of measurement geometries for multi-angle spectrophotometers", Color Res. Appl., 36 (2011) *in press*.

[34] S. Kitaguchi, M.R. Luo, S. Westland, E.J.J. Kirchner and G.J. van den Kieboom, "Assessing texture difference for metallic coating on different media", Proc. IS&T/SID's Fourteenth Color Imaging Conference, Scottsdale, pg. 197-202. (2006).

[35] S. Kitaguchi, S. Westland, M.R. Luo, E.J.J. Kirchner and G.J. van den Kieboom, "Application of HDR Imaging to Modeling of Glints in Metallic Coatings", Proc. AIC 2008 Interim Meeting Colour – Effects & Affects, Stockholm. (2008).

[36] B. Han, M.R. Luo and E.J.J. Kirchner, "Assessing colour differences for automobile coatings using CRT colours part II: evaluating colour difference of textured colours", Proc. 10th Congress of the International Colour Association (AIC), Granada, pg. 583-586. (2005).

[37] W. Ji, M. R. Luo and E. Kirchner, "Assessing colour apperance and colour differences for automobile coatings- methods for assessing coarseness", Proc. 10th Congress of the International Colour Association (AIC), Granada, pg. 631-634. (2005).

[38] R. Huertas, M. Melgosa and E. Hita, "Parametric factors for colour differences of samples with simulated texture", Proc. 10th Congress of the International Colour Association (AIC), Granada, pg. 631–634. (2005).

[39] E.D. Montag and R.S. Berns, "Lightness dependencies and the effect of texture on suprathreshold lightness tolerances", Color Res. Appl., 25, 241–249 (2000).

[40] J.H. Xin, H.L. Shen and C.C. Lam, “Investigation of texture effect on visual colour difference evaluation”, Color Res. Appl., 30, 341–347 (2005).

Author biography

Eric Kirchner received his MSc in theoretical physics at the University of Utrecht, and a PhD in chemistry at the Free University of Amsterdam. Since 2000 he works as a scientist specialized in colorimetry, for the Automotive and Aerospace Coatings division in AkzoNobel. His research topics include: color and texture perception, accurate rendering of color and texture, optical modeling and color difference equations.